IEEE Access
Multidisciplinary | Rapid Review | Open Access Journal

Received 20 March 2024, accepted 8 April 2024, date of publication 10 April 2024, date of current version 19 April 2024.

Digital Object Identifier 10.1109/ACCESS.2024.3387024

RESEARCH ARTICLE

ML-Based Forecasting of Temporal Dynamics in Luminescence Spectra of Ag_2S Colloidal Quantum Dots

IVAN P. MALASHIN[1], DANIIL S. DAIBAGYA[2,3], VADIM S. TYNCHENKO[1,4], (Senior Member, IEEE), VLADIMIR A. NELYUB[1,5], ALEKSEI S. BORODULIN[1], ANDREI P. GANTIMUROV[1], SERGEY A. AMBROZEVICH[2,3], AND ALEXANDR S. SELYUKOV[2,3]

[1]Artificial Intelligence Technology Scientific and Education Center, Bauman Moscow State Technical University, 105005 Moscow, Russia
[2]Faculty of Fundamental Science, Bauman Moscow State Technical University, 105005 Moscow, Russia
[3]P. N. Lebedev Physical Institute, Russian Academy of Sciences, 119991 Moscow, Russia
[4]Information-Control Systems Department, Institute of Computer Science and Telecommunications, Reshetnev Siberian State University of Science and Technology, 660037 Krasnoyarsk, Russia
[5]Scientific Department, Far Eastern Federal University, 690922 Vladivostok, Russia

Corresponding author: Ivan P. Malashin (ivan.p.malashin@gmail.com)

ABSTRACT The study delves into the temporal dynamics of luminescence in colloidal Ag_2S quantum dots, utilizing time series forecasting techniques. Through an analysis of intensity measurements taken at different time intervals, it uncovers temporal trends and utilizes predictive models to anticipate future behaviour of luminescence spectra. The outcomes contribute to a more profound understanding of optimizing experimental conditions and foreseeing the evolution of these nanomaterials over time. Among the tested models, the most robust and effective approaches for predicting the decay of integral intensity within the first hour include polynomial features with regressors, particularly ElasticNetCV, Ridge, and Lasso, with R^2 scores of 0.74, 0.82, and 0.80, respectively. However, upon comparison with the results of additional experiment conducted over a duration of two hours, the Ridge model demonstrated the best performance in predicting the decay of integral intensity.

INDEX TERMS Machine learning, Ag_2S, quantum dots, luminescence, time series, temporal dynamics, prediction.

I. INTRODUCTION

In recent years, the intersection of quantum dot research and machine learning [1], [2] has emerged as a pivotal frontier, fostering advancements in both nanotechnology and artificial intelligence. Quantum dots (QDs), nanoscale semiconductor particles, exhibit unique size-dependent optical and electronic properties, making them promising candidates for applications ranging from bioimaging to quantum computing. Harnessing the full potential of QD requires a deep understanding of their complex behavior, and this has prompted the integration of machine learning (ML) methodologies to unravel intricate patterns and unlock hidden insights within vast datasets.

The associate editor coordinating the review of this manuscript and approving it for publication was Larbi Boubchir.

In the literature, there are numerous examples illustrating the integration of QD with ML techniques. For example, work [2] addresses the challenges of tuning and scaling large-scale quantum devices, especially in QD-based architectures. Deep convolutional neural networks (CNN) are employed to characterize states and charge configurations of semiconductor QD arrays based on currentvoltage characteristics of transport. Study [3] addresses the challenge of limited and inconsistent data in nanomaterials synthesis by employing ML to predict outcomes of InP QD syntheses. Work [4] demonstrates a significant advancement in semiconductor QD devices by employing a machine learning algorithm and optimization routine for experimental tuning, particularly crucial for applications like quantum computing. Utilizing machine learning, specifically Bayesian optimization, the study [1] not only optimizes synthesis for monodispersity

FIGURE 1. Visualization of promising application areas for Ag_2S QD.

but also provides insights beyond the original parameter space, guiding strategies for further improvements in PbS CQD synthesis. Paper [5] emphasizes the conventional time-consuming nature of materials development and introduces the Materials Genome Initiative (MGI) to expedite the process through computational tools and experimental platforms. Machine learning is highlighted as a powerful tool within MGI, showcasing its potential to accelerate material discovery, predict structures, and optimize material properties and performance of QD. In the realm of large-scale semiconductor-based qubit initialization, the automated tuning of gate-defined QD is crucial, requiring charge-state detection based on charge stability diagrams. Article [6] evaluates the prediction accuracy of ML models, emphasizing the necessity of realistic QD simulations and noise models for effective charge-state detection using supervised machine learning. Significance of developing mathematical models for predicting the optical band gap energy of zinc oxide (ZnO) nanostructures to expedite the production of ZnO-based devices is highlighted in [7]. The implementation of supervised machine learning, particularly Kernel Ridge Regression (KRR) with quadratic features, and Artificial Neural Network (ANN), is showcased for accurate prediction, revealing the potential of machine learning models in automating semiconductor property predictions to accelerate materials design and applications. The developed ML algorithm in [8], utilizing normalized spectral and time-resolved photoluminescence (PL) data of CdTe QD emission, demonstrates a significant advancement by achieving accuracies in low and high-temperature regimes, howcases the potential of machine learning to accurately sense temperature in microfluidic and nanofluidic devices.

The compound Ag_2S (silver(I) sulfide) is of significant importance in the field of functional nanomaterials, such as:

- **Optical Properties:** Ag_2S exhibits unique optical properties, particularly in the infrared spectrum [9], making it a crucial material for applications in optical technology, especially for infrared detectors and photonics.
- **Semiconductor Characteristics:** Ag_2S is a semiconductor, and its electronic properties can be effectively tuned for use in electronics and semiconductor devices [10].
- **Photosensitivity:** Due to its photosensitivity in the visible and near-infrared spectrum, Ag_2S is of interest in photovoltaics and solar cells [11].
- **Structure and Morphology:** The structure [12] and morphology of Ag_2S can be modified into nanostructures such as nanoparticles [13], [14] and nanowires [15]. These nanostructures can be integrated into functional nanomaterials to create new properties and possibilities in nanotechnology.

ML techniques, driven by algorithms capable of learning and adapting from data, offer a powerful toolkit for analyzing and predicting QD temporal dynamics [16]. This synergistic approach aims to bridge the gap between theoretical models and experimental observations, providing a more comprehensive understanding of QD dynamics.

Fig.1 illustrates showcases diverse sectors, including electronics, optics, medicine, energy, environmental science, materials research, scientific exploration, future technolo-

gies, agriculture, and transportation, where Ag_2S QD are anticipated to make significant contributions.

In electronics, they exhibit potential for developing materials and devices with enhanced electronic characteristics [17], [18], [19]. Their utilization in optics allows for the creation of novel materials applicable in sensors [20], and other optical devices [21].

In the medical field, Ag_2S QD demonstrate promise in the development of biomedical technologies such as cell labeling, diagnostics, and tumor therapy [22], [23]. Their unique optical and electronic properties make them attractive for applications in disease detection and treatment. [24]

In the energy sector, Ag_2S QD can be used to create new materials in solar cells and other devices [25] aimed at efficiently harnessing solar energy [26]. They may also find applications in environmental science, contributing to the development of effective methods for water and air purification.

In materials science, Ag_2S QD provide unique opportunities for creating new materials with improved properties [27].

The application of Ag_2S QD in sensors represents a promising avenue for detecting various pollutants in the air, water, and soil [28]. It makes a significant contribution to environmental monitoring, ensuring reliable detection and control of various pollutants.

Ag_2S offer size-tunable energy levels [29] and quantum confinement effects [30], [31], making them suitable for qubits in quantum information processing [32]. Their long coherence times [33], compatibility with diverse materials [34], and efficient light-matter interaction position them for integration into quantum processors and quantum communication devices.

Undoubtedly, Ag_2S QD represent unique research objects with prospects for applications in various fields, making them a subject of heightened interest in modern science and technology.

We posit that a robust machine learning models can effectively capture the complex nonlinear patterns inherent in the spectral data, thereby enabling accurate prediction of integral intensity dynamics over time. Central to our methodology are the machine learning models utilized for spectral prediction. We employ a diverse ensemble of regression algorithms, including but not limited to ElasticNetCV, AdaBoost, Bagging, and CatBoost.

By emphasizing precision and signal integrity, we presents an innovative perspective in the realm of photoluminescence modeling. The aim of this study is to assess and identify optimal predictive ML models for the temporal dynamics of luminescence degradation in colloidal Ag_2S QD.

II. THEORETICAL FRAMEWORK

In numerous systems, the decay behavior exhibits complexity, characterized by slower-than-exponential decay. The decline of the wideband emission progresses much more gradually than an exponential decay, and over extended durations, it assumes a stretched exponential (SE) pattern $\exp\left[\frac{-(t/t_c)^\beta}{\beta}\right]$, with an exponent of $\beta = 0.5$ and a characteristic time $t_c = 240$ ns [35]. SE tail aligns with the distribution of relaxation times, as depicted by the integral of $h(t)\,\mathrm{d}\,t$, as described in [36].

$$h(t)\,\mathrm{d}\,t = \frac{\beta}{(1-\beta)\cdot\Gamma\left(\frac{1-\beta}{\beta}\right)\tau_{ch}}\exp\left[-(t/t_c)^{\beta/(1-\beta)}\right]$$

where G represents the gamma function. In simpler terms, the observed value $\beta = 0.5$ suggests that the trap states exhibit a straightforward exponential distribution of lifetimes.

For instance, when considering a luminescent decay modeled as a sum of exponential processes characterized by a distribution of relaxation times $h(t)$, normalized such that $\int_0^1 h(t)dt = 1$, and the duration of the excitation pulse is short compared to the fastest relaxation time in the spectrum, the photoluminescent decay $S_p(t)$ can be expressed as [35]:

$$S_p(t) = \int_0^t \tau^{-1} e^{-\frac{t}{\tau}} h(\tau)\,\mathrm{d}\,\tau$$

where the radiated light is normalized such that $\int_0^1 S_p(t)dt = 1$. The arithmetic average relaxation time τ_0 is then calculated as $\int_0^1 tS_p(t)dt$.

While such models provide valuable insights, they are often complex and computationally intensive. This motivates the exploration of machine learning techniques, which offer the potential to approximate these complex nonlinear and dynamic models with more lightweight alternatives for faster predictive modeling.

Therefore, it is hypothesized that machine learning models can effectively approximate the behavior of luminescence decay, capturing the essential features of the underlying processes while reducing computational complexity. By leveraging machine learning algorithms, it is anticipated that predictive solutions can be generated more efficiently, facilitating rapid analysis and interpretation of luminescence data.

III. MATERIALS AND METHODS

A. EXPERIMENTAL SETUP

The Ag_2S nanoparticles were synthesized using the technique of photoinduced growth in ethylene glycol, providing passivation of their surface with 2-mercaptopropionic acid [37]. Silver nitrate was used as the silver source and 2-mercaptopropionic acid (2-MPA) taken in molar ratio twice the amount of silver nitrate was used as the sulfur source. The synthesis was carried out in a glass flask thermostated at 25 Â°C and under constant stirring with a magnetic stirrer. 2.4 mmol of silver nitrate was placed in 30 mL of ethylene glycol and then 4.8 mmol of 2-mercaptopropionic acid was added also as a solution in ethylene glycol. The growth of nanoparticles was carried out in a dark room overnight. Reduction of the size dispersion of the resulting nanoparticles was realized by photolysis by irradiating the resulting solution with 405 nm laser irradiation and an

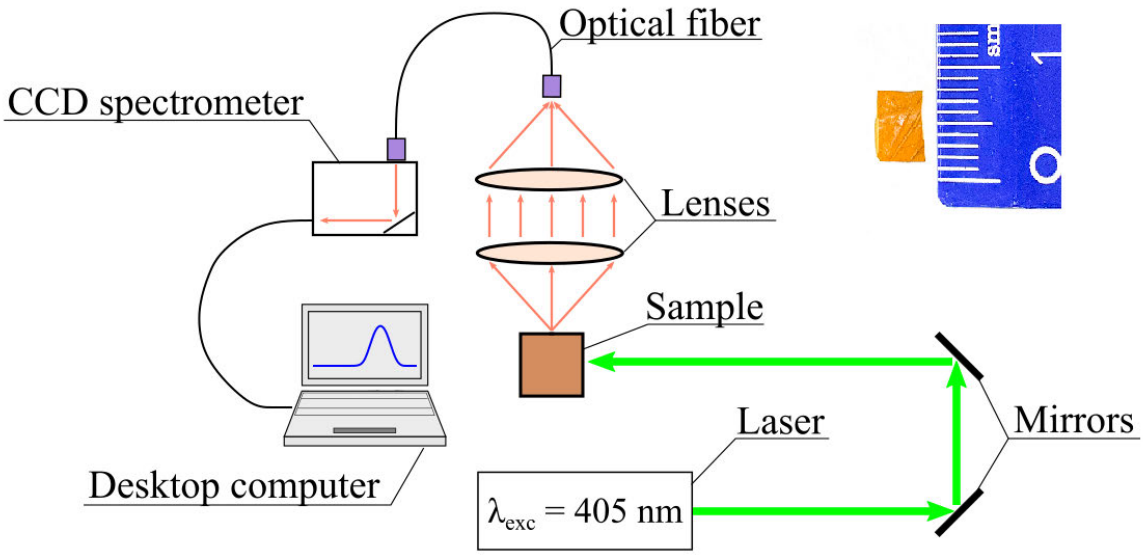

FIGURE 2. Experimental setup. The inset shows a photograph of QD embedded in a dielectric matrix.

average power of 100 mW under constant stirring for a day. After the photolysis procedure, the nanoparticles were kept in the dark for three days for stabilization.

Further in-depth insights into the characteristics and properties of Ag_2S/2-MPA colloidal QD can be gleaned from comprehensive studies available in the papers [37], [38], [39]. These publications delve into the intricate synthesis methodologies, structural analyses, and unique optical and electronic behaviors exhibited by Ag_2S/2-MPA QD.

The nanoparticles were embedded by infiltration of the resulting solution into an optically passive dielectric organic matrix based on a 5 μm thick semipermeable membrane made of regenerated cellulose (the inset of Fig. 2); the characteristic pore sizes of the membrane were of the order of 3 nm. To record photoluminescence spectra, QD embedded in a dielectric organic matrix were clamped between two glasses.

Fig. 2 shows a schematic of the experimental setup for measuring the photoluminescence spectra of QD. The light source (was PicoQuant LDH-C 400 pulsed laser (excitation wavelength: $\lambda_{exc} = 405$ nm; pulse duration: $\Delta\tau = 75$ ps; repetition rate: $\nu = 40$ MHz). Laser radiation was redirected using mirrors to the sample. The luminescence of the sample was focused using two lenses with a focal distance of 10 cm and collected by an optical fiber. Luminescence was transferred to an Ocean Optics Maya 2000Pro CCD spectrometer, which was connected to a desktop computer. Photoluminescence spectra of QD were recorded under continuous laser irradiation for 1 hour. Similar experimental setups for studying the photoluminescence of QD can be found in the work of [40].

Morphology of the synthesized colloidal QD was studied with the use of a Libra 120 transmission electron microscope (TEM).

The absorption spectrum of the colloidal solution of Ag_2S nanoparticles was recorded with a Perkin-Elmer Lambda 45 spectrophotometer with an operating wavelength range of 190…1100 nm and a spectral resolution of 1 nm.

B. MORPHOLOGY AND OPTICAL PROPERTIES

The synthesized QD were characterized with the use of the transmission electron microscopy (Fig. 3). Fig. 3 shows the TEM images of the synthesized nanocrystals. The samples are ensembles of Ag_2S colloidal QD. The size distribution of nanoparticles is presented by histograms The histogram indicates the formation of Ag_2S QDs with an average diameter of 2.6-2.7 nm and a dispersion of 40%.

Fig.4 shows the absorption spectrum of the colloidal QD. The spectral band has a large width and a feature. The maximum of this feature is centered at the energy 1.80 eV. This feature corresponds to the interband absorption [41]. In the framework of the strong confinement approximation [42], using the effective mass approximation, we can estimate the average size of colloidal QD from the blue shift of the exciton absorption band maximum in the ground state. For this purpose, let's use Brus's expression [42]:

$$E_g^{QDs} = E_g^{bulk} + \frac{\hbar^2\pi^2}{2\mu R^2} - \frac{1.8e^2}{\varepsilon R}.$$

Here, E_g^{QDs} is the QD band gap value, $E_g^{bulk} = 1.0$ eV is the bulk crystal band gap [43], [44], R is the QD radius, $\varepsilon = 5.95$ is the permittivity [45], $\mu = m_e m_h/(m_e + m_h)$ is the reduced mass, $m_e = 0.42m_0$ and $m_h = 0.81m_0$ are electron and hole effective masses [46]. The average diameter of the investigated QD was 2.61 nm, which correlates well with the TEM study.

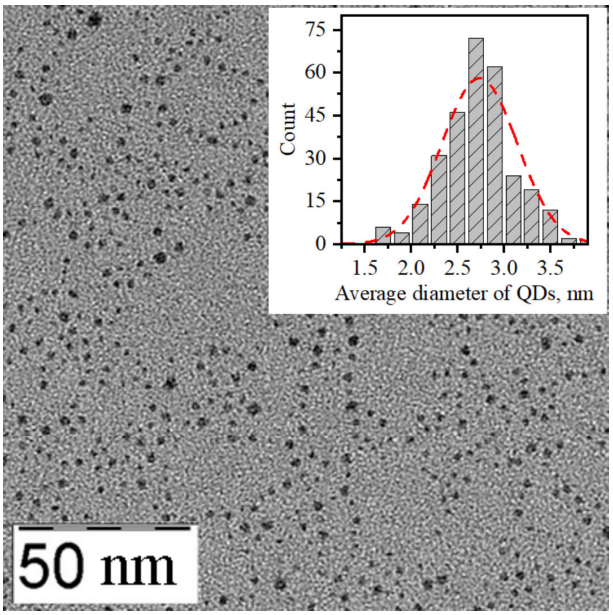

FIGURE 3. TEM image of the synthesized colloidal QD. The inset shows the size distribution histogram of QDs and the Gaussian distribution fit to the data.

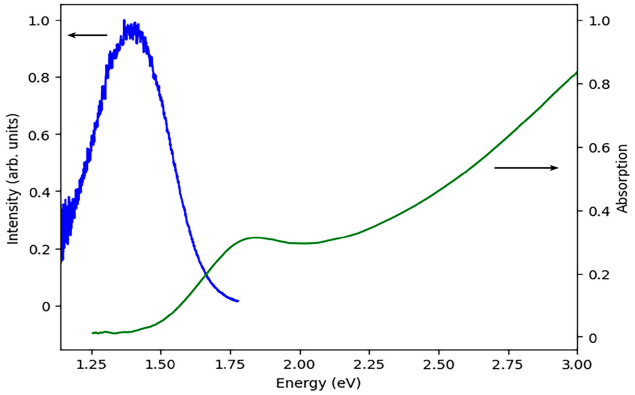

FIGURE 4. Absorption and photoluminescence spectra of Ag_2S colloidal QD.

Photoluminescence spectrum of Ag_2S/2-MPA colloidal QD is shown in the Fig.4. The emission peak was centered at 1.38 eV. The full width at half maximum (FWHM) was 0.31 eV. This emission spectrum is associated with trap-state luminescence and corresponds to the 2.61 nm Ag_2S QD [47]. The maxima of the photoluminescence and absorption spectra of colloidal Ag_2S/2-MPA QD are shifted to the short-wavelength region relative to the bulk Ag_2S crystal, which is due to the quantum confinement effect.

C. DATASET PROCESSING

In this study, we focused on the processing of a dataset containing fluorescence spectra of Ag_2S at various time points, specifically recording information every 0.5 seconds over the course of one hour using a spectrometer. The recorded parameters included energy (E) and intensity (I(E)).

The data processing pipeline involves the following steps:

1) Importing necessary libraries including os, pandas, curve_fit from scipy.optimize, and numpy.
2) Defining the Gaussian function for curve fitting.
3) Setting the path to the folder containing the.txt spectra files.
4) Creating an empty DataFrame to store the results.
5) Iterating through each file and fitting selected range of spectra by Gaussian function using curve_fit.
6) Appending the Gaussian coefficients (A, B, C) as the results to the DataFrame.
7) Utilizing various polynomial regressors to explore the potential behavior of these Gaussian coefficients over the next hour.
8) Analyzing the trends and patterns observed in the coefficients to gain insights into the dynamic changes in the spectral data.
9) Assessing the predictive performance of the polynomial regression models in capturing the temporal dynamics of the Gaussian coefficients.
10) Comparing the performance of different polynomial regressors based on metrics such as mean squared error, R-squared value, and visual inspection of predicted versus actual values.

To approximate the photoluminescence spectrum, we employed a Gaussian function $A \cdot e^{-(x-B)^2/C^2}$ that corresponds to radiative transitions from traps [48], where A is amplitude (Intensity) of the Gaussian function, B is energy at which the intensity reaches its maximum, C is FWHM. To mitigate noise in the raw data and improve the accuracy of the photoluminescence spectrum approximation, Gaussian function fitting was performed for signal data within the energy range of 1.16 to 1.8 eV. This specific range was chosen as substantial noise was consistently observed, typically falling between 1.1 to 1.2 eV on each graph 2. By avoiding the noisy regions during the Gaussian fitting process, the approximation is less influenced by erratic fluctuations or artifacts in the data. This ensures that the extracted Gaussian parameters (A, B, C) more accurately represent the true characteristics of the photoluminescence signal. A similar operation was conducted for all 7180 records, enabling us to capture the dynamics of Gaussian coefficients (A, B, C) over time. Subsequently, employing machine learning methods, particularly time series techniques, we forecasted the dynamics of these coefficients for the next three hours.

Among the diverse time series techniques explored in this study, Polynomial Features [49] stood out as the most effective method for capturing the underlying physics of the Ag_2S fluorescence spectra dynamics over time. Polynomial Features is a feature engineering technique that, when applied to time series data, generates polynomial combinations of the original features, allowing the model to better capture non-linear relationships. This method proved particularly adept at handling the intricate and non-linear dependencies present in the dataset, resulting in superior forecasting accuracy.

In contrast, other well-established time series techniques, including Autoregressive Integrated Moving Average (ARIMA) [50], Seasonal Decomposition of Time Series (STL) [51], Prophet [52], Exponential Smoothing State Space Models (ETS) [53], Long Short-Term Memory (LSTM) Networks [54], Gated Recurrent Unit (GRU) Networks [55], XGBoost and LightGBM [56], Dynamic Time Warping (DTW) [57], Hybrid Models [58], Bayesian Structural Time Series (BSTS) [59], and Ensemble Methods [60], did not yield comparable success in capturing the nuances of the Ag_2S fluorescence spectra.

Application of more traditional methods, such as polynomial regressions, might provide more interpretable and accurate results for the analysis of Ag_2S temporal dynamics.

The inadequacy of these techniques can be attributed to the specific characteristics of the dataset, such as complex non-linear dependencies [61], intricate seasonal patterns, and the need for capturing long-term dependencies. Some models, like ARIMA and ETS, struggled to adapt to the non-linear dynamics, while others, such as LSTM and GRU networks, faced challenges in effectively capturing the long-term dependencies present in the fluorescence spectra.

Moreover, models like XGBoost and LightGBM, which require feature engineering to convert time series data into a tabular format, were less suited for the unique structure of the dataset. Despite their popularity, these methods could not overcome the inherent complexities present in the Ag_2S fluorescence spectra dataset.

Fig. 5 illustrates experiment pipeline designed [62] to ascertain the optimal interval for approximating original data with a Gaussian function, followed by the extraction of coefficients. Our methodology involves employing various Machine Learning Time Forecasting techniques to forecast the coefficients A, B, and C of the Gaussian approximations. To determine the most suitable forecasting method, we conduct a thorough examination by utilizing 30 distinct regressors and experimenting with different polynomial degrees. This systematic analysis aims to identify the optimal configuration, providing valuable insights into the polynomial features that effectively capture the underlying patterns in our Gaussian approximations. The selection of the best regressor and polynomial degree is crucial for accurate forecasting. As a result, we observe diffrent luminescence degradation scenarios in Ag_2S QD, highlighting the significance of the chosen forecasting technique in predicting [63] the temporal evolution of QD behavior.

In summary, the success of Polynomial Features underscores the importance of tailored feature engineering methods for specific datasets, highlighting the limitations of conventional time series techniques in capturing the intricate dynamics of Ag_2S fluorescence spectra. Among the various regressors utilized, they can be broadly categorized into several classes based on their underlying algorithms [64] and functionalities. All regressor mentioned in Appendix.

The choice of different polynomial degrees provided the flexibility to adapt the model to more complex nonlinear dependencies in the data [65]. For instance, with a degree of 9, the model could account for high-level nonlinear effects, which might be crucial for accurately predicting changes in Gaussian coefficients.

However, it is worth noting that higher polynomial degrees also increase the risk of overfitting [66], especially with a limited amount of data. In the context of this study, using degrees 2-9 struck a balance between capturing complex dependencies and preventing overfitting, making the model more flexible and capable of adapting to the dynamics of coefficient changes in the spectra.

This exploration of regressor categories highlights the versatility and adaptability of the `PolynomialFeatures` method. In order to develop predictive models for the target coefficients, a systematic approach was adopted, involving the partitioning of the dataset into training and testing sets. This division, implemented with an 80-20 split (80% for training and 20% for testing), ensures a robust evaluation of model performance [67]. Employing diffrent Regression modeling techniques like in paper [68], a various-degree polynomial was chosen, allowing for flexibility in capturing non-linear relationships within the data. The features were transformed using Polynomial Features to introduce polynomial terms, and an each Regression model was trained for each target coefficient. This modeling strategy is designed to extract and encapsulate intricate patterns inherent in the data, fostering accurate predictions of the target coefficients. The resulting models, represented by instances of various regressors and the corresponding polynomial transformations, are poised to contribute valuable insights into the nuanced relationships between features and target gaussian coefficients.

IV. RESULTS

Fig. 6 illustrates the temporal evolution of coefficients A, B, and C, comparing the actual data to the predictions made by various models over a span of one hour.

Additionally, it showcases the best forecasts for each coefficient extending into the subsequent hour of the coefficients approximating Gaussian functions, mimicking the dynamic behavior of the luminescence spectra of Ag_2S QD. The visual representation captures the efficacy of the forecasting models in capturing the nuanced changes in the coefficients, offering a valuable tool for understanding and predicting the temporal dynamics of these nanomaterials.

In Fig. 7, the comparison between real Spectra and Gaussian Approximations over 600-Second Intervals.

Notably, the Gaussian approximations, both individually tailored for each time point and those with coefficients modeled using PolynomialFeatures (ElasticNetCV regressor with a degree of 2), exhibit an alignment within the margin of error. This close correspondence is particularly evident in the context of the inherent noise present in the original data, showcasing the robustness of the modeling approach. The agreement between the approximated profiles and those modeled with PolynomialFeatures and ElasticNetCV

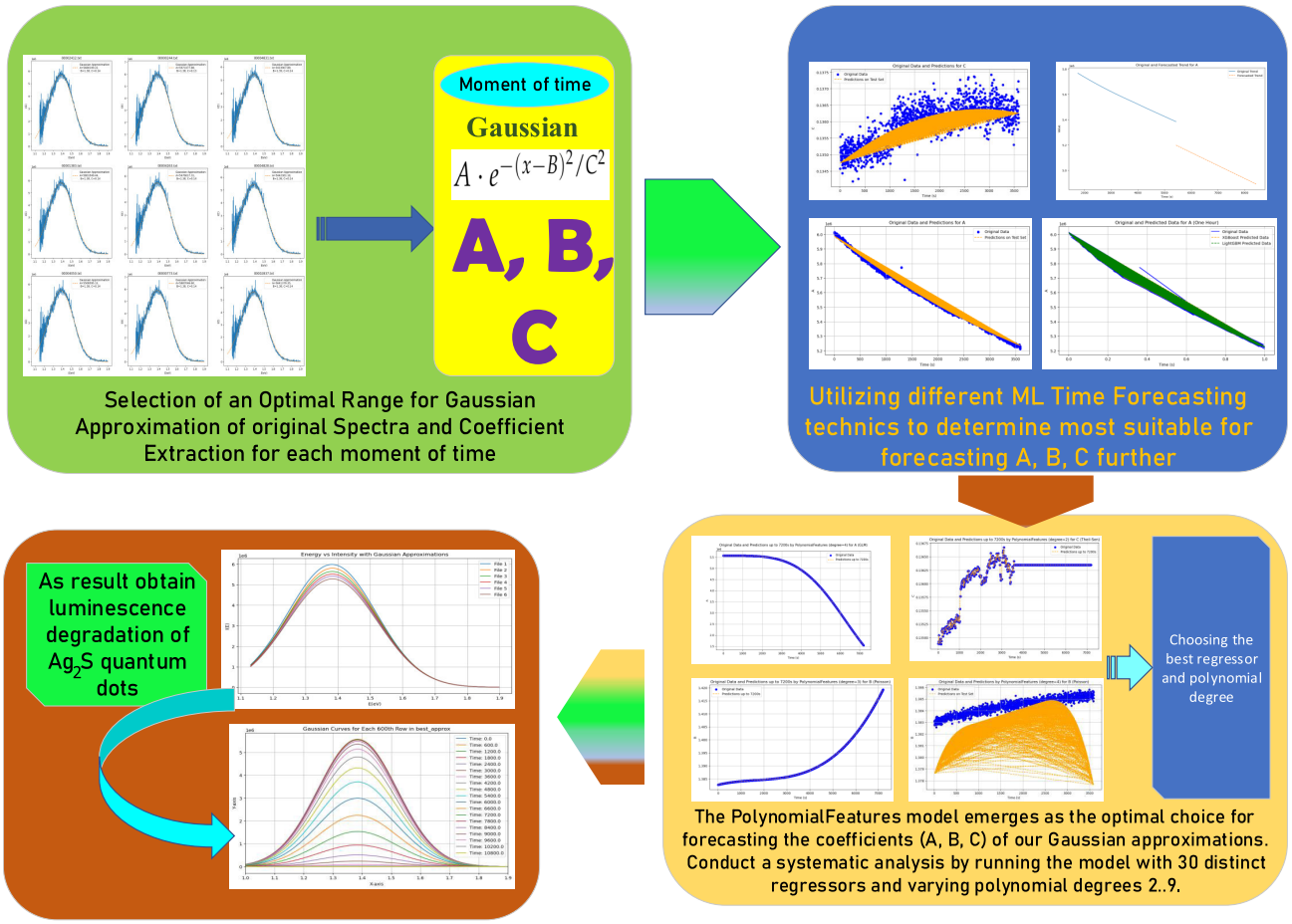

FIGURE 5. Experiment pipeline.

underscores the reliability of the obtained results. These findings further emphasize the practical convergence of the Gaussian representations.

Fig. 8 a) depicts the approximations of the initial spectra using Gaussian curves, with the areas beneath each curve shaded accordingly. These approximations reflect the temporal evolution of the emission intensity of Ag_2S QD. The shaded areas under the Gaussian curves illustrate how the ingral intensity changes over time. Additionally, the inset provides numerical values for the corresponding areas, offering a more detailed assessment of the dynamics of emission intensity throughout the experiment.

In Fig. 8 b) illustrates Temporal Evolution of integral intensity: Comparison between the experimentally observed and predicted integral intensity over time. The blue curve represents the integral intensity derived from initial data, while the orange, green and red curves depicts the integral intensity predicted using PolynomialFeatures with regressor ElasticNetCV, Ridge and Lasso with polynomial degre 2, 2, 3 respectively.

These extended curves provide a glimpse into potential scenarios for the degradation of luminescence in Ag_2S QD over a two-hour period. To address the presentation of results we conducted an additional experiment to observe the decay of the integral intensity of Ag_2S quantum dots. Unlike the initial experiment which lasted for one hour, this extended experiment spanned over two hours (Fig. 8b, lightgreen curve). The results revealed that the decay behavior was slower than exponential, indicating the presence of complex dynamics.

Furthermore, we compared the predictions generated by the Ridge regression model with the observed decay behavior. Remarkably, the Ridge model accurately captured the slower decay dynamics, aligning well with the experimental observations. This direct comparison between the model predictions and real data underscores the validity and significance of the Ridge regression approach in capturing the nuanced behavior of the integral intensity decay.

V. DISCUSSION

In our investigation of various regression models for predicting the integral intensity over time, we have uncovered distinct behaviors in their performance. Certainly, the Ridge regression model notably demonstrated an almost linear decay of the initial data, suggesting a trend that smoothly traverses through all the original data points. In contrast, the

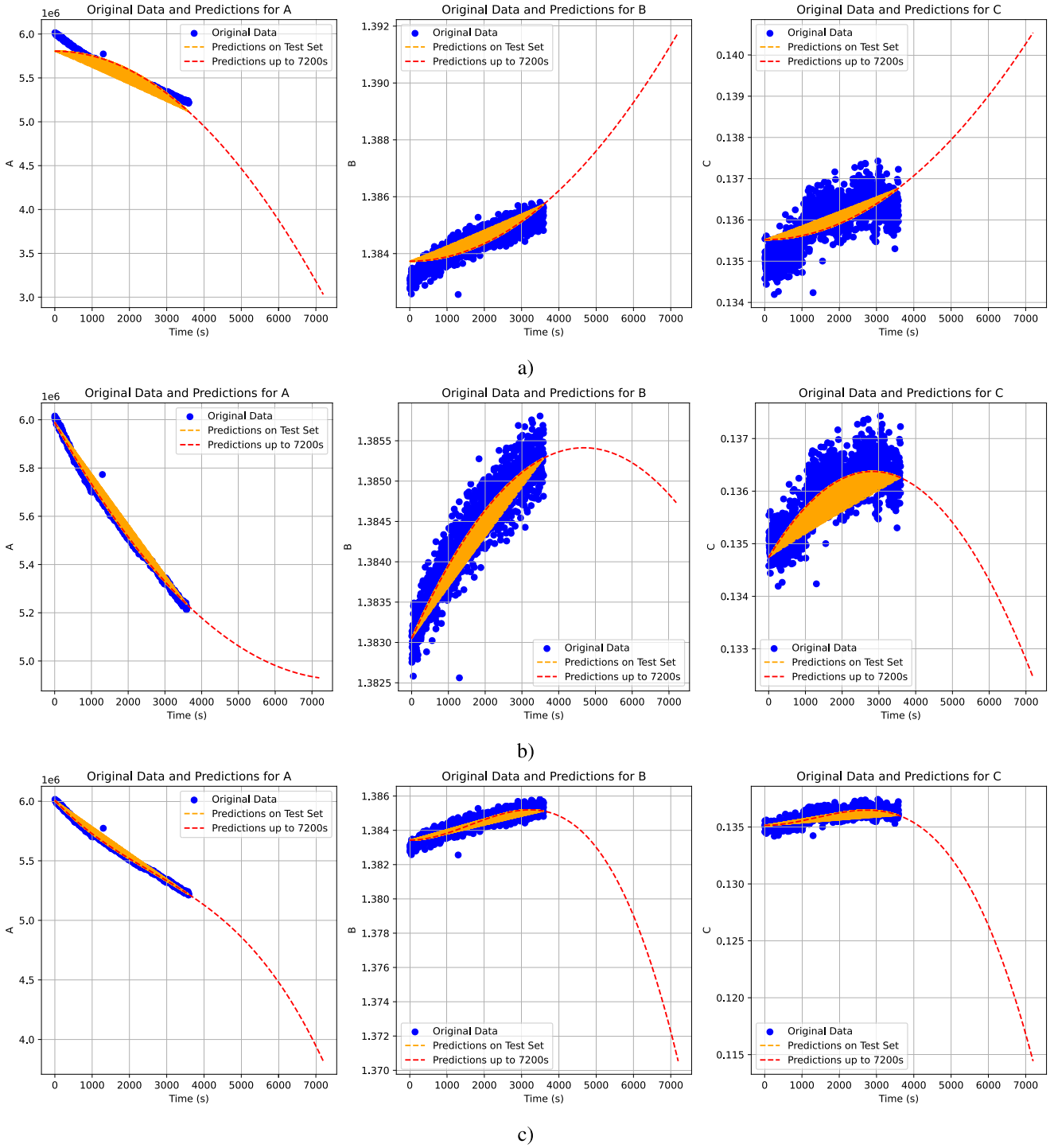

FIGURE 6. **Temporal evolution of coefficients A, B, and C: real vs. predicted data over 1 hour (3600 s) and best forecast for the following hour (up to 7200 s) for regressor a) ElasticNetCV b) Ridge c) Lasso with polynomial degre 2, 2, 3 respectively.**

ElasticNet and Lasso models exhibited a downward trend. Specifically, the ElasticNet model displayed a parabolic shape, diverging from a linear fit, whereas the Ridge model showcased a polynomial behavior that encompassed all original data points, indicating a slower rate of decline compared to ElasticNet. Additionally, both the ElasticNet and Lasso models exhibited an upward convexity, which contradicts the slower-than-exponential decay pattern observed in the data.

Understanding the reasons behind model behavior is a key aspect of result analysis and can help explain differences in their predictions. Here are several possible aspects to consider for a better understanding of model behavior:

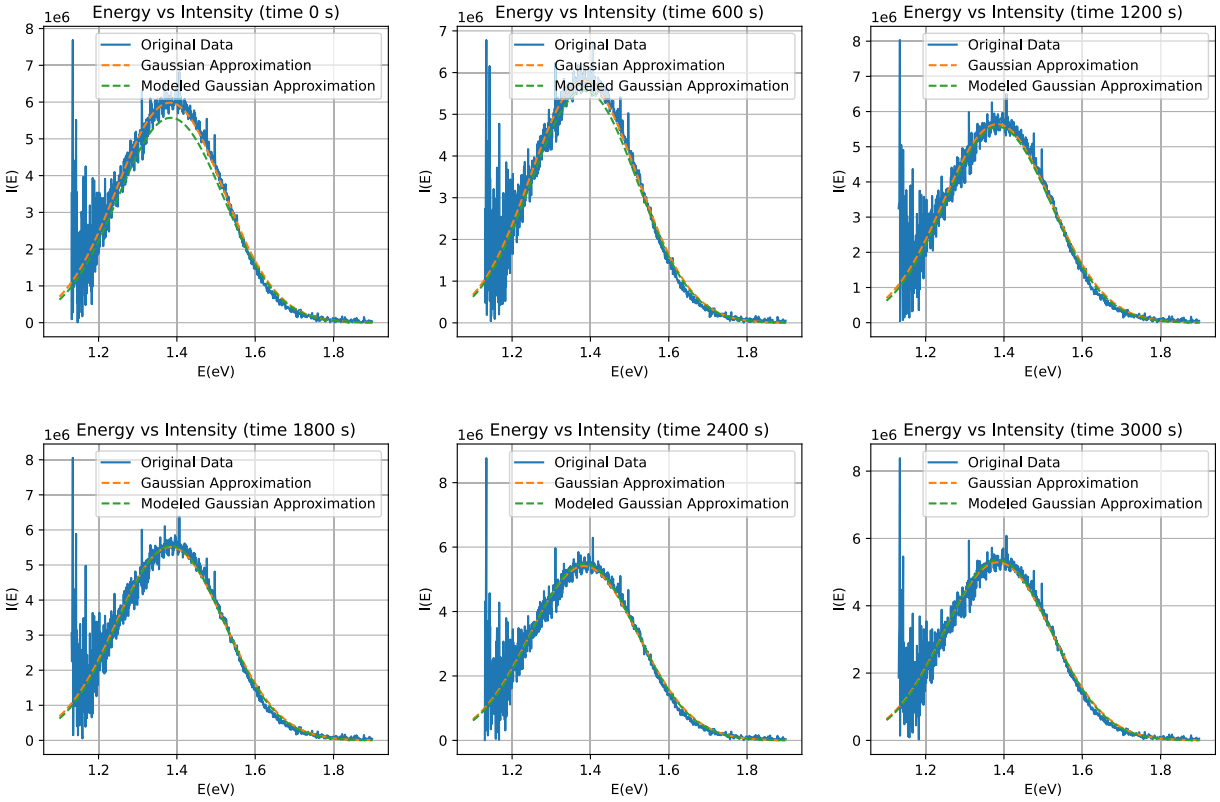

FIGURE 7. Temporal evolution of spectral profiles.

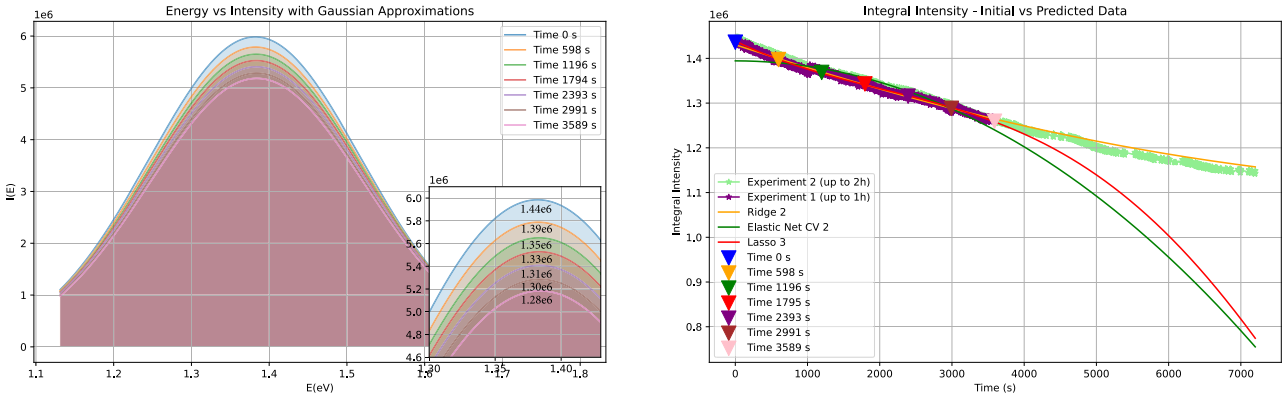

a) b)

FIGURE 8. a) Gaussian approximations of initial spectra with shaded areas representing changing emission intensity over time. Inset values provide a detailed view of integral intensity dynamics. b) Temporal evolution of integral intensity: Comparison between observed and predicted areas. Blue curve: Initial data; Orange: ElasticNetCV (deg=2), Green: Ridge (deg=2), Red: Lasso (deg=3). Insights into agreement between experimental and predicted trends.

different regularization approaches and sensitivity to outliers and nonlinear dependencies.

Regularization plays a crucial role in controlling the complexity of machine learning models and preventing overfitting. There are various approaches to regularization, each of which introduces unique adjustments to the model training process. For example, Ridge regression adds a quadratic penalty term to the loss function, reducing the magnitude of coefficients and preventing overfitting. In contrast, Lasso regression applies L1 regularization, leading to feature selection and potentially setting some coefficients to zero, making the model more interpretable and robust to multicollinearity. ElasticNet, on the other hand, combines both L1 and L2 regularization, striking a balance between feature selection and preventing overfitting. Each of these approaches has its own advantages and disadvantages, and the choice of a specific method depends on the characteristics of the data and the desired level of interpretability of the model.

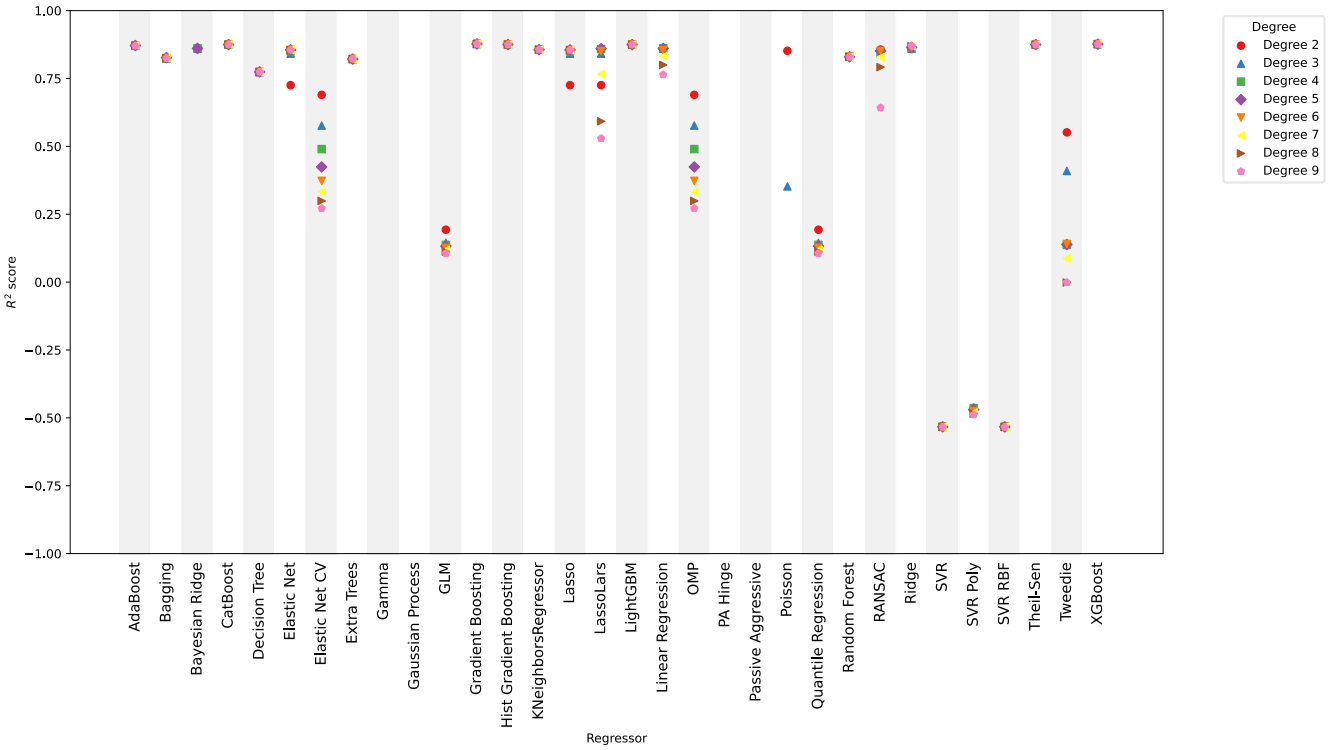

FIGURE 9. R^2 score for coefficient a in various regression models at different degrees of the regressor.

The sensitivity of machine learning models to outliers and nonlinear dependencies is an important aspect of their application in real-world tasks. Some models may be more robust to outliers and better able to handle nonlinear dependencies in the data. For example, the Ridge regression model, due to its quadratic penalty, is less sensitive to outliers compared to Lasso regression, which uses L1 regularization and can set some coefficients to zero. However, Lasso regression may be less effective in modeling nonlinear dependencies in the data due to its feature selection property. ElasticNet, which combines both regularization methods, offers a compromise approach that can provide a balance between robustness to outliers and the ability of the model to capture nonlinear relationships in the data.

Furthermore, an intriguing observation arises from our analysis, where the most optimal models consistently yield decreasing curves for the Gaussian area. This behavior aligns with the physical intuition that the intensity of fluorescence spectra tends to diminish over time. Notably, alternative models occasionally produced counterintuitive outcomes, indicating an increase in the Gaussian area, which contradicts the expected physical behavior. Such discrepancies may stem from inherent complexities in the interplay of the underlying processes, challenging the models' ability to generalize effectively.

Fig. 9 compares R^2 metrics for coefficient A in different regression models at various degrees of the regressor. R^2, or the coefficient of determination, provides crucial insights into the quality of model fitting to the data. In an ideal fit, the R^2 value is equal to 1. However, if all metrics for one regressor at different degrees are equal to 1, it may indicate overfitting.

Overfitting [69] occurs when the model overly tailors itself to the training data, including its noise and random variations, making it incapable of generalizing to new data. In such cases, a high R^2 is observed, but the model will struggle to predict new values accurately. Therefore, analyzing R^2 metrics at different degrees of the regressor allows assessing the optimal complexity of the model and avoiding overfitting.

Conversely, when the R^2 value is too low, it signals insufficient learning [70] of the model from the provided data. Poor model fitting quality can lead to non-physical behavior in predicting coefficients, making it less reliable in various practical scenarios. Thus, the R^2 metric becomes a key tool in evaluating the balance between model complexity and its ability to generalize to new data, providing an optimal representation of the physical properties of the system

In some instances, certain models resulted in predicted curves represented by horizontal lines, indicating a lack of sensitivity to the temporal evolution of the Gaussian area. This behavior raises questions about the model's ability to capture the nuanced dynamics and adapt to variations in the underlying physical processes. Potential reasons for this phenomenon may include insufficient complexity in the chosen models, underfitting of the training data, or the neglect of critical features influencing the Gaussian area.

The diverse outcomes underscore the importance of not only selecting the most accurate model but also choosing one that aligns with the expected physical behavior. The

exploration of regression models in predicting Gaussian area dynamics provides valuable insights into the challenges and nuances of capturing intricate temporal patterns in fluorescence spectra.

VI. CONCLUSION

In conclusion, our exploration of time series forecasting techniques for predicting the dynamic evolution of Gaussian parameters in fluorescence spectra unveils the intricate relationship between model selection and physical interpretability. While various substances may exhibit unique behaviors necessitating tailored modeling approaches, our study establishes a robust framework for uncovering the temporal nuances in fluorescence dynamics.

The identified best models of PolynomialFeatures with diffrent regressors, such as Lasso, ElasticNet, and Ridge, emerge as promising candidates for predicting Gaussian area changes, demonstrating their capacity to align with the expected physical trends. These findings suggest that the proposed methodologies could serve as valuable tools in unraveling the time-dependent characteristics of fluorescence spectra for a wide range of substances.

The broader implications of our work extend beyond the specific case of Ag_2S fluorescence, providing a roadmap for researchers in different domains to navigate the intricate landscape of time series modeling. By addressing the challenges and nuances associated with predicting dynamic changes in Gaussian parameters, our study contributes to the development of versatile methodologies applicable to diverse spectral datasets. As we embark on further investigations into different materials, the insights gleaned from this research pave the way for advancing our understanding of complex temporal phenomena across various scientific disciplines.

Future Directions for this work can include:

1) **Feature Engineering:** Investigate additional features or engineered features derived from employing various approximation methods for the spectra of different quantum dots, potentially altering the dataset and improving model performance. This process may require domain-specific expertise to identify pertinent predictors capable of more accurately capturing the underlying patterns within the data.
2) **Model Optimization:** Continuously refine and optimize the ML models by experimenting with different algorithms, hyperparameters, and ensemble methods. Techniques such as cross-validation and grid search can be employed to identify the best-performing model configurations.
3) **Incorporating Temporal Dynamics:** Develop models that explicitly capture the temporal dynamics of the integral intensity over time. Time series forecasting methods, recurrent neural networks (RNNs), or attention mechanisms can be explored to handle sequential data and dependencies between observations.
4) **Integration with Domain Knowledge:** Incorporate domain knowledge from luminescence physics or materials science into the modeling process. This could involve integrating physical constraints or insights into the ML algorithms to improve the interpretability and accuracy of the forecasts.
5) **Validation and Evaluation:** Conduct comprehensive validation and evaluation of the ML models using rigorous statistical methods. This includes assessing model performance on unseen data, conducting sensitivity analyses, and evaluating the robustness of the models to different scenarios or perturbations.
6) **Deployment and Integration:** Explore methods for deploying the trained ML models into practical applications, such as real-time monitoring systems or decision support tools. Integration with existing infrastructure or workflows may require additional considerations such as scalability, reliability, and interpretability.
7) **Interdisciplinary Collaboration:** Foster collaboration between researchers from diverse fields such as physics, materials science, computer science, and statistics. Collaborative efforts can lead to novel insights, interdisciplinary approaches, and more holistic solutions to complex problems in luminescence forecasting.
8) **Exploration of Alternative Techniques:** Investigate alternative techniques beyond traditional ML approaches, such as deep learning, reinforcement learning, or Bayesian methods. These techniques may offer advantages in handling complex data structures, non-linear relationships, or uncertainty quantification.
9) **Addressing Data Limitations:** Overcome challenges associated with data collection, which may arise due to constraints or limitations inherent in the experimental setup.

APPENDIX
DATA AVAILABILITY

The code implementing the described experiments is available in the repository at QuantumDots-Luminescence-Dynamics. Researchers and enthusiasts can access, review, and contribute to the codebase for further exploration and collaboration.

APPENDIX
UTILIZED REGRESSION MODELS

1) **Traditional Regression Models:**
   - **Linear Regression:** Utilizes a linear approach to model the relationship between the independent and dependent variables [71].
   - **Ridge Regression:** Addresses multicollinearity by introducing regularization to the linear regression model [72].
   - **Lasso Regression:** Incorporates L1 regularization, encouraging sparsity in the regression coefficients [73].
   - **Elastic Net:** Combines L1 and L2 regularization to overcome limitations of Lasso and Ridge [74].

- **LARS Lasso:** Performs Lasso regression using the Least Angle Regression algorithm [75].
- **Huber Regressor:** Robust regression model that combines qualities of both mean squared error and mean absolute error [76].
- **RANSAC Regressor:** Robustly fits a linear regression model to data with a significant presence of outliers [77].
- **Orthogonal Matching Pursuit (OMP):** Iteratively selects features that most correlate with the target variable [78].
- **Theil-Sen Regressor:** Robust method for estimating the slope of a linear regression model [79].

2) **Ensemble Models:**
- **Bagging Regressor:** Constructs multiple models and combines their predictions to reduce overfitting [80].
- **Adaboost Regressor:** Boosting algorithm that focuses on the weaknesses of preceding models [81].
- **Gradient Boosting Regressor:** Builds an additive model sequentially, each correcting errors of the previous one [82].
- **Random Forest Regressor:** Ensemble of decision trees with random feature selection [83].
- **Stacking Regressor:** Combines multiple regression models to improve overall performance [84].
- **Extra Trees Regressor:** Similar to a random forest but with additional randomness in the feature selection process [85].
- **HistGradient Boosting Regressor:** Optimized version of gradient boosting that uses histograms for splitting [86].

3) **Support Vector Machines (SVM) Regressors:**
- **Support Vector Regressor (SVR) with Linear Kernel:** Utilizes linear kernel for SVM-based regression [87].
- **SVR with Polynomial Kernel:** Applies a polynomial kernel to capture nonlinear relationships [88].
- **SVR with Radial Basis Function (RBF) Kernel:** Uses radial basis functions to map input data into higher-dimensional space [89].

4) **Advanced Models:**
- **K-Nearest Neighbors (KNN) Regressor:** Predicts the target variable based on the average of its k-nearest neighbors [90].
- **Decision Tree Regressor:** Models decisions as a tree structure, splitting data based on feature conditions [91].
- **XGBoost Regressor:** Gradient boosting algorithm known for its speed and performance [92].
- **CatBoost Regressor:** Gradient boosting algorithm designed for categorical features [93].
- **LightGBM Regressor:** Gradient boosting framework that uses tree-based learning [94].
- **Gaussian Process Regressor:** Models the target variable distribution using Gaussian processes [95].
- **Bayesian Ridge Regression:** Applies Bayesian methods to linear regression [96].
- **Kernel Ridge Regressor:** Combines ridge regression with the kernel trick for nonlinear relationships [97].
- **Gamma Regressor:** Models the gamma distribution [98].

REFERENCES

[1] O. Voznyy, L. Levina, J. Z. Fan, M. Askerka, A. Jain, M.-J. Choi, O. Ouellette, P. Todorovic, L. K. Sagar, and E. H. Sargent, "Machine learning accelerates discovery of optimal colloidal quantum dot synthesis," *ACS Nano*, vol. 13, no. 10, pp. 11122–11128, Oct. 2019.

[2] S. S. Kalantre, J. P. Zwolak, S. Ragole, X. Wu, N. M. Zimmerman, M. D. Stewart, and J. M. Taylor, "Machine learning techniques for state recognition and auto-tuning in quantum dots," *npj Quantum Inf.*, vol. 5, no. 1, p. 6, Jan. 2019.

[3] H. A. Nguyen, F. Y. Dou, N. Park, S. Wu, H. Sarsito, B. Diakubama, H. Larson, E. Nishiwaki, M. Homer, M. Cash, and B. M. Cossairt, "Predicting indium phosphide quantum dot properties from synthetic procedures using machine learning," *Chem. Mater.*, vol. 34, no. 14, pp. 6296–6311, Jul. 2022.

[4] J. P. Zwolak, S. S. Kalantre, X. Wu, S. Ragole, and J. M. Taylor, "QFlow lite dataset: A machine-learning approach to the charge states in quantum dot experiments," *PLoS ONE*, vol. 13, no. 10, Oct. 2018, Art. no. e0205844.

[5] J. Peng, R. Muhammad, S. Wang, and H. Zhong, "How machine learning accelerates the development of quantum dots?" *Chin. J. Chem.*, vol. 39, no. 1, pp. 181–188, Jan. 2021.

[6] J. Darulová, M. Troyer, and M. C. Cassidy, "Evaluation of synthetic and experimental training data in supervised machine learning applied to charge-state detection of quantum dots," *Mach. Learn., Sci. Technol.*, vol. 2, no. 4, Dec. 2021, Art. no. 045023.

[7] P. R. Regonia, C. M. Pelicano, R. Tani, A. Ishizumi, H. Yanagi, and K. Ikeda, "Predicting the band gap of ZnO quantum dots via supervised machine learning models," *Optik*, vol. 207, Apr. 2020, Art. no. 164469.

[8] C. Lewis, J. W. Erikson, D. A. Sanchez, C. E. McClure, G. P. Nordin, T. R. Munro, and J. S. Colton, "Use of machine learning with temporal photoluminescence signals from CdTe quantum dots for temperature measurement in microfluidic devices," *ACS Appl. Nano Mater.*, vol. 3, no. 5, pp. 4045–4053, May 2020.

[9] I. Ezenwa, N. Okereke, and N. Egwunyenga, "Optical properties of chemical bath deposited Ag_2S thin films," *Int. J. Sci. Technol.*, vol. 2, no. 3, pp. 101–106, 2012.

[10] R. Zamiri, H. Abbastabar Ahangar, A. Zakaria, G. Zamiri, M. Shabani, B. Singh, and J. M. F. Ferreira, "The structural and optical constants of Ag_2S semiconductor nanostructure in the far-infrared," *Chem. Central J.*, vol. 9, no. 1, pp. 1–6, Dec. 2015.

[11] J. Xue, J. Liu, S. Mao, Y. Wang, W. Shen, W. Wang, L. Huang, H. Li, and J. Tang, "Recent progress in synthetic methods and applications in solar cells of Ag_2S quantum dots," *Mater. Res. Bull.*, vol. 106, pp. 113–123, Oct. 2018.

[12] S. I. Sadovnikov, M. G. Kostenko, A. I. Gusev, and A. V. Lukoyanov, "Low-temperature predicted structures of Ag_2S (Silver Sulfide)," *Nanomaterials*, vol. 13, no. 19, p. 2638, Sep. 2023.

[13] A. I. Kryukov, A. L. Stroyuk, N. N. Zin'chuk, A. V. Korzhak, and S. Y. Kuchmii, "Optical and catalytic properties of Ag_2S nanoparticles," *J. Mol. Catal. A, Chem.*, vol. 221, nos. 1–2, pp. 209–221, Nov. 2004.

[14] Y. Ma, Z. Zhao, Y. Xian, H. Wan, Y. Ye, L. Chen, H. Zhou, and J. Chen, "Highly dispersed Ag_2S nanoparticles: In situ synthesis, size control, and modification to mechanical and tribological properties towards nanocomposite coatings," *Nanomaterials*, vol. 9, no. 9, p. 1308, Sep. 2019.

[15] X. Wen, S. Wang, Y. Xie, X.-Y. Li, and S. Yang, "Low-temperature synthesis of single crystalline Ag_2S nanowires on silver substrates," *J. Phys. Chem. B*, vol. 109, no. 20, pp. 10100–10106, May 2005.

[16] M. Ryo, C. A. Aguilar-Trigueros, L. Pinek, L. A. H. Müller, and M. C. Rillig, "Basic principles of temporal dynamics," *Trends Ecol. Evol.*, vol. 34, no. 8, pp. 723–733, Aug. 2019.

[17] G. M. Neelgund, S. F. Aguilar, E. A. Jimenez, and R. L. Ray, "Adsorption efficiency and photocatalytic activity of silver sulfide nanoparticles deposited on carbon nanotubes," *Catalysts*, vol. 13, no. 3, p. 476, Feb. 2023.

[18] A. Badawi, "Effect of the non-toxic Ag_2S quantum dots size on their optical properties for environment-friendly applications," *Phys. E, Low-Dimensional Syst. Nanostruct.*, vol. 109, pp. 107–113, May 2019.

[19] S. Daibagya Daniil, S. A. Ambrozevich, A. S. Perepelitsa, I. A. Zakharchuk, A. V. Osadchenko, D. M. Bezverkhnyaya, A. I. Avramenko, and A. S. Selyukov, "Spectral and kinetic properties of silver sulfide quantum dots in an external electric field," *J. Sci. Tech. Inf. Technol., Mech. Opt.*, vol. 146, no. 6, p. 1098, 2022.

[20] J. Feng, Y. Qian, Q. Cheng, Y. Ma, D. Wu, H. Ma, X. Ren, X. Wang, and Q. Wei, "A signal amplification of p DNA@Ag_2S based photoelectrochemical competitive sensor for the sensitive detection of OTA in microfluidic devices," *Biosensors Bioelectron.*, vol. 168, Nov. 2020, Art. no. 112503.

[21] A. Badawi and S. S. Alharthi, "Controlling the optical and mechanical properties of polyvinyl alcohol using Ag_2S semiconductor for environmentally friendly applications," *Mater. Sci. Semicond. Process.*, vol. 116, Sep. 2020, Art. no. 105139.

[22] T. Jamieson, R. Bakhshi, D. Petrova, R. Pocock, M. Imani, and A. M. Seifalian, "Biological applications of quantum dots," *Biomaterials*, vol. 28, no. 31, pp. 4717–4732, 2007.

[23] R. E. Bailey, A. M. Smith, and S. Nie, "Quantum dots in biology and medicine," *Phys. E, Low-Dimensional Syst. Nanostruct.*, vol. 25, no. 1, pp. 1–12, 2004.

[24] Y. Zhang, G. Hong, Y. Zhang, G. Chen, F. Li, H. Dai, and Q. Wang, "Ag_2S quantum dot: A bright and biocompatible fluorescent nanoprobe in the second near-infrared window," *ACS Nano*, vol. 6, no. 5, pp. 3695–3702, May 2012.

[25] S. Chand, E. Sharma, and P. Sharma, "Phase change induced quantization in NIR emitting Ag_2S nanocrystals: Structural and optical response for solar energy applications," *J. Alloys Compounds*, vol. 770, pp. 1173–1180, Jan. 2019.

[26] X. Guo, J. Gao, Z. Zhang, S. Xiao, D. Pan, C. Zhou, J. Shen, J. Hong, and Y. Yang, "Highly efficient interfacial layer using SILAR-derived Ag_2S quantum dots for solid-state bifacial dye-sensitized solar cells," *Mater. Today Energy*, vol. 5, pp. 320–330, Sep. 2017.

[27] C. Ding, Y. Huang, Z. Shen, and X. Chen, "Synthesis and bioapplications of Ag_2S quantum dots with near-infrared fluorescence," *Adv. Mater.*, vol. 33, no. 32, 2021, Art. no. 2007768.

[28] H. Xu, J. Li, Y. Fu, P. Li, W. Luo, and Y. Tian, "Ag/Ag_2S nanoparticle-induced sensitization of recovered sulfur-doped SnO_2 nanoparticles for SO_2 detection," *ACS Appl. Nano Mater.*, vol. 3, no. 8, pp. 8075–8087, Aug. 2020.

[29] M. K. Ali, S. Javaid, H. Afzal, I. Zafar, K. Fayyaz, Q. U. Ain, M. A. Rather, M. J. Hossain, S. Rashid, K. A. Khan, and R. Sharma, "Exploring the multifunctional roles of quantum dots for unlocking the future of biology and medicine," *Environ. Res.*, vol. 232, Sep. 2023, Art. no. 116290.

[30] Y. Zhang, Y. Liu, C. Li, X. Chen, and Q. Wang, "Controlled synthesis of Ag_2S quantum dots and experimental determination of the exciton bohr radius," *J. Phys. Chem. C*, vol. 118, no. 9, pp. 4918–4923, Mar. 2014.

[31] D. S. Daibagya, I. A. Zakharchuk, A. V. Osadchenko, A. S. Selyukov, S. A. Ambrozevich, M. L. Skorikov, and R. B. Vasiliev, "Luminescence and colorimetric properties of ultrathin cadmium selenide nanoscrolls," *Bull. Lebedev Phys. Inst.*, vol. 50, no. 11, pp. 510–514, Nov. 2023.

[32] N. T. Kalyani, S. J. Dhoble, M. M. Domanska, B. Vengadaesvaran, H. Nagabhushana, and A. K. Arof, *Quantum Dots: Emerging Materials for Versatile Applications*. Sawston, U.K.: Woodhead Publishing, 2023.

[33] T. S. Kondratenko, A. I. Zvyagin, M. S. Smirnov, I. G. Grevtseva, A. S. Perepelitsa, and O. V. Ovchinnikov, "Luminescence and nonlinear optical properties of colloidal Ag_2S quantum dots," *J. Lumin.*, vol. 208, pp. 193–200, Apr. 2019.

[34] B. Mukherjee, M. Saxena, Y.-K. Kuo, G. S. Okram, S. Dam, S. Hussain, A. Lakhani, U. Deshpande, and T. Shripathi, "Ag-nanoinclusion-induced enhanced thermoelectric properties of Ag_2S," *ACS Appl. Energy Mater.*, vol. 2, no. 9, pp. 6383–6394, Sep. 2019.

[35] L. E. Shea-Rohwer and J. E. Martin, "Luminescence decay of broadband emission from CdS quantum dots," *J. Lumin.*, vol. 127, no. 2, pp. 499–507, Dec. 2007.

[36] J. E. Martin and L. E. Shea-Rohwer, "Lifetime determination of materials that exhibit a stretched exponential luminescent decay," *J. Lumin.*, vol. 121, no. 2, pp. 573–587, Dec. 2006.

[37] O. V. Ovchinnikov, S. V. Aslanov, M. S. Smirnov, I. G. Grevtseva, and A. S. Perepelitsa, "Photostimulated control of luminescence quantum yield for colloidal Ag_2S/2-MPA quantum dots," *RSC Adv.*, vol. 9, no. 64, pp. 37312–37320, 2019.

[38] O. Ovchinnikov, S. Aslanov, M. Smirnov, A. Perepelitsa, T. Kondratenko, A. Selyukov, and I. Grevtseva, "Colloidal Ag_2S/SiO_2 core/shell quantum dots with IR luminescence," *Opt. Mater. Exp.*, vol. 11, no. 1, pp. 89–104, 2021.

[39] A. I. Zvyagin, T. A. Chevychelova, K. S. Chirkov, M. S. Smirnov, and O. V. Ovchinnikov, "Nonlinear optical properties of colloidal PbS and Ag_2S quantum dots passivated with 2-mercaptopropionic acid," *Bull. Russian Acad. Sci., Phys.*, vol. 86, no. 10, pp. 1183–1187, Oct. 2022.

[40] D. S. Daibagya, "Spectral and kinetic characteristics of ultrathin cadmium selenide nanoscrolls," *Sci. Tech. J. Inf. Technol., Mech. Opt.*, vol. 23, no. 5, pp. 920–926, Oct. 2023.

[41] O. V. Ovchinnikov, M. S. Smirnov, B. I. Shapiro, T. S. Shatskikh, A. S. Perepelitsa, and N. V. Korolev, "Optical and structural properties of ensembles of colloidal Ag_2S quantum dots in gelatin," *Semiconductors*, vol. 49, no. 3, pp. 373–379, Mar. 2015.

[42] L. Brus, "Electronic wave functions in semiconductor clusters: Experiment and theory," *J. Phys. Chem.*, vol. 90, no. 12, pp. 2555–2560, Jun. 1986.

[43] W. Jiang, Z. Wu, X. Yue, S. Yuan, H. Lu, and B. Liang, "Photocatalytic performance of Ag_2S under irradiation with visible and near-infrared light and its mechanism of degradation," *RSC Adv.*, vol. 5, no. 31, pp. 24064–24071, 2015.

[44] S. Liu, X. Wang, W. Zhao, K. Wang, H. Sang, and Z. He, "Synthesis, characterization and enhanced photocatalytic performance of Ag_2S-coupled ZnO/ZnS core/shell nanorods," *J. Alloys Compounds*, vol. 568, pp. 84–91, Aug. 2013.

[45] X. Lu, L. Li, W. Zhang, and C. Wang, "Preparation and characterization of Ag_2S nanoparticles embedded in polymer fibre matrices by electrospinning," *Nanotechnology*, vol. 16, no. 10, pp. 2233–2237, Oct. 2005.

[46] S. Lin, Y. Feng, X. Wen, P. Zhang, S. Woo, S. Shrestha, G. Conibeer, and S. Huang, "Theoretical and experimental investigation of the electronic structure and quantum confinement of wet-chemistry synthesized Ag_2S nanocrystals," *J. Phys. Chem. C*, vol. 119, no. 1, pp. 867–872, Jan. 2015.

[47] D. S. Daibagya, S. A. Ambrozevich, and A. S. Perepelitsa, "Electric field influence on the recombination luminescence of the colloidal silver sulfide quantum dots," *Herald Bauman Moscow State Tech. Univ., Natural Sci.*, vol. 3, no. 108, pp. 100–117, 2023.

[48] M. S. Smirnov and O. V. Ovchinnikov, "IR luminescence mechanism in colloidal Ag_2S quantum dots," *J. Lumin.*, vol. 227, Nov. 2020, Art. no. 117526.

[49] F. Dubosson, S. Bromuri, and M. Schumacher, "A Python framework for exhaustive machine learning algorithms and features evaluations," in *Proc. IEEE 30th Int. Conf. Adv. Inf. Netw. Appl. (AINA)*, Mar. 2016, pp. 987–993.

[50] B. K. Nelson, "Time series analysis using autoregressive integrated moving average (ARIMA) models," *Academic Emergency Med.*, vol. 5, no. 7, pp. 739–744, Jul. 1998.

[51] M. Theodosiou, "Forecasting monthly and quarterly time series using STL decomposition," *Int. J. Forecasting*, vol. 27, no. 4, pp. 1178–1195, Oct. 2011.

[52] C. Saiktishna, N. S. V. Sumanth, M. M. S. Rao, and J. Thangakumar, "Historical analysis and time series forecasting of stock market using FB prophet," in *Proc. 6th Int. Conf. Intell. Comput. Control Syst. (ICICCS)*, May 2022, pp. 1846–1851.

[53] R. Hyndman, A. B. Koehler, J. K. Ord, and R. D. Snyder, *Forecasting With Exponential Smoothing: The State Space Approach*. Berlin, Germany: Springer, 2008.

[54] S. Egan, W. Fedorko, A. Lister, J. Pearkes, and C. Gay, "Long short-term memory (LSTM) networks with jet constituents for boosted top tagging at the LHC," 2017, *arXiv:1711.09059*.

[55] R. Dey and F. M. Salem, "Gate-variants of gated recurrent unit (GRU) neural networks," in *Proc. IEEE 60th Int. Midwest Symp. Circuits Syst. (MWSCAS)*, Aug. 2017, pp. 1597–1600.

[56] E. Al Daoud, "Comparison between XGBoost, LightGBM and CatBoost using a home credit dataset," *Int. J. Comput. Inf. Eng.*, vol. 13, no. 1, pp. 6–10, 2019.
[57] H. Li, "Time works well: Dynamic time warping based on time weighting for time series data mining," *Inf. Sci.*, vol. 547, pp. 592–608, 2021.
[58] Y. Gala, Á. Fernández, J. Díaz, and J. R. Dorronsoro, "Hybrid machine learning forecasting of solar radiation values," *Neurocomputing*, vol. 176, pp. 48–59, Feb. 2016.
[59] J. Qiu, S. R. Jammalamadaka, and N. Ning, "Multivariate Bayesian structural time series model," *J. Mach. Learn. Res.*, vol. 19, no. 1, pp. 2744–2776, 2018.
[60] T. G. Dietterich, "Ensemble methods in machine learning," in *Proc. Int. Workshop Multiple Classifier Syst.* Berlin, Germany: Springer, 2000, pp. 1–15.
[61] I. S. Masich, V. S. Tyncheko, V. A. Nelyub, V. V. Bukhtoyarov, S. O. Kurashkin, and A. S. Borodulin, "Paired patterns in logical analysis of data for decision support in recognition," *Computation*, vol. 10, no. 10, p. 185, Oct. 2022.
[62] V. S. Tynchenko, S. O. Kurashkin, V. V. Tynchenko, V. V. Bukhtoyarov, V. V. Kukartsev, R. B. Sergienko, S. V. Tynchenko, and K. A. Bashmur, "Software to predict the process parameters of electron beam welding," *IEEE Access*, vol. 9, pp. 92483–92499, 2021.
[63] I. S. Masich, V. S. Tynchenko, V. A. Nelyub, V. V. Bukhtoyarov, S. O. Kurashkin, A. P. Gantimurov, and A. S. Borodulin, "Prediction of critical filling of a storage area network by machine learning methods," *Electronics*, vol. 11, no. 24, p. 4150, Dec. 2022.
[64] A. Mikhalev, V. Tynchenko, V. Nelyub, N. Lugovaya, V. Baranov, V. Kukartsev, R. Sergienko, and S. Kurashkin, "The orb-weaving spider algorithm for training of recurrent neural networks," *Symmetry*, vol. 14, no. 10, p. 2036, Sep. 2022.
[65] A. Gasparrini, "Distributed lag linear and non-linear models inR: The packagedlnm," *J. Stat. Softw.*, vol. 43, no. 8, p. 1, 2011.
[66] S. Yeom, I. Giacomelli, M. Fredrikson, and S. Jha, "Privacy risk in machine learning: Analyzing the connection to overfitting," in *Proc. IEEE 31st Comput. Secur. Found. Symp. (CSF)*, Jul. 2018, pp. 268–282.
[67] W. Brendel, J. Rauber, M. Kümmerer, I. Ustyuzhaninov, and M. Bethge, "Accurate, reliable and fast robustness evaluation," in *Proc. Adv. Neural Inf. Process. Syst.*, vol. 32, 2019.
[68] I. P. Malashin, V. S. Tynchenko, V. A. Nelyub, A. S. Borodulin, and A. P. Gantimurov, "Estimation and prediction of the polymers' physical characteristics using the machine learning models," *Polymers*, vol. 16, no. 1, p. 115, Dec. 2023. [Online]. Available: https://www.mdpi.com/2073-4360/16/1/115
[69] D. M. Hawkins, "The problem of overfitting," *J. Chem. Inf. Comput. Sci.*, vol. 44, no. 1, pp. 1–12, Jan. 2004.
[70] D. Scanlon, "Specific learning disability and its newest definition: Which is comprehensive? And which is insufficient?" *J. Learn. Disabilities*, vol. 46, no. 1, pp. 26–33, Jan. 2013.
[71] S. Weisberg, *Applied Linear Regression*, vol. 528. Hoboken, NJ, USA: Wiley, 2005.
[72] G. C. McDonald, "Ridge regression," *Wiley Interdiscipl. Rev. Comput. Stat.*, vol. 1, no. 1, pp. 93–100, 2009.
[73] J. Ranstam and J. Cook, "LASSO regression," *J. Brit. Surg.*, vol. 105, no. 10, p. 1348, 2018.
[74] A. R. Atilgan, S. R. Durell, R. L. Jernigan, M. C. Demirel, O. Keskin, and I. Bahar, "Anisotropy of fluctuation dynamics of proteins with an elastic network model," *Biophys. J.*, vol. 80, no. 1, pp. 505–515, Jan. 2001.
[75] S. Sathiya Keerthi and S. Shevade, "A fast tracking algorithm for generalized LARS/LASSO," *IEEE Trans. Neural Netw.*, vol. 18, no. 6, pp. 1826–1830, Nov. 2007.
[76] S. Balasundaram and Y. Meena, "Robust support vector regression in primal with asymmetric Huber loss," *Neural Process. Lett.*, vol. 49, no. 3, pp. 1399–1431, Jun. 2019.
[77] R. Subbarao and P. Meer, "Beyond RANSAC: User independent robust regression," in *Proc. Conf. Comput. Vis. Pattern Recognit. Workshop (CVPRW)*, Jun. 2006, p. 101.
[78] Y. C. Pati, R. Rezaiifar, and P. S. Krishnaprasad, "Orthogonal matching pursuit: Recursive function approximation with applications to wavelet decomposition," in *Proc. 27th Asilomar Conf. Signals, Syst. Comput.*, Nov. 1993, pp. 40–44.
[79] R. Wilcox, "A note on the Theil-Sen regression estimator when the regressor is random and the error term is heteroscedastic," *Biometrical J., J. Math. Methods Biosci.*, vol. 40, no. 3, pp. 261–268, 1998.
[80] L. Breiman, "Bagging predictors," *Mach. Learn.*, vol. 24, no. 2, pp. 123–140, Aug. 1996.
[81] S. Patil, A. Patil, and V. M. Phalle, "Life prediction of bearing by using Adaboost regressor," in *Proc. TRIBOINDIA-Int. Conf. Tribol.*, 2018, pp. 1–8.
[82] A. Kadiyala and A. Kumar, "Applications of Python to evaluate the performance of bagging methods," *Environ. Prog. Sustain. Energy*, vol. 37, pp. 1555–1559, 2018.
[83] M. R. Segal, *Machine Learning Benchmarks and Random Forest Regression*. San Francisco, CA, USA: Center for Bioinformatics and Molecular Biostatistics, 2004.
[84] S. Acharya, D. Swaminathan, S. Das, K. Kansara, S. Chakraborty, D. Kumar R, T. Francis, and K. R. Aatre, "Non-invasive estimation of hemoglobin using a multi-model stacking regressor," *IEEE J. Biomed. Health Informat.*, vol. 24, no. 6, pp. 1717–1726, Jun. 2020.
[85] S. M. Mastelini, F. K. Nakano, C. Vens, and A. C. P. de Leon Ferreira de Carvalho, "Online extra trees regressor," *IEEE Trans. Neural Netw. Learn. Syst.*, vol. 34, no. 10, pp. 6755–6767, Oct. 2023.
[86] R. Gayathri, S. U. Rani, L. Čepová, M. Rajesh, and K. Kalita, "A comparative analysis of machine learning models in prediction of mortar compressive strength," *Processes*, vol. 10, no. 7, p. 1387, Jul. 2022.
[87] S. Kavitha, S. Varuna, and R. Ramya, "A comparative analysis on linear regression and support vector regression," in *Proc. Online Int. Conf. Green Eng. Technol. (IC-GET)*, Nov. 2016, pp. 1–5.
[88] C. López-Martín, M. Azzeh, A. Bou-Nassif, and S. Banitaan, "Upsilon-SVR polynomial kernel for predicting the defect density in new software projects," in *Proc. 17th IEEE Int. Conf. Mach. Learn. Appl. (ICMLA)*, Dec. 2018, pp. 1377–1382.
[89] Z. Ramedani, M. Omid, A. Keyhani, S. Shamshirband, and B. Khoshnevisan, "Potential of radial basis function based support vector regression for global solar radiation prediction," *Renew. Sustain. Energy Rev.*, vol. 39, pp. 1005–1011, Nov. 2014.
[90] O. Kramer and O. Kramer, "K-nearest neighbors," in *Dimensionality Reduction With Unsupervised Nearest Neighbors*. Berlin, Germany: Springer, 2013, pp. 13–23.
[91] M. Xu, P. Watanachaturaporn, P. Varshney, and M. Arora, "Decision tree regression for soft classification of remote sensing data," *Remote Sens. Environ.*, vol. 97, no. 3, pp. 322–336, Aug. 2005.
[92] S. K. Patel, J. Surve, V. Katkar, J. Parmar, F. A. Al-Zahrani, K. Ahmed, and F. M. Bui, "Encoding and tuning of THz metasurface-based refractive index sensor with behavior prediction using XGBoost regressor," *IEEE Access*, vol. 10, pp. 24797–24814, 2022.
[93] M. Arora, A. Sharma, S. Katoch, M. Malviya, and S. Chopra, "A state of the art regressor Model's comparison for effort estimation of agile software," in *Proc. 2nd Int. Conf. Intell. Eng. Manage. (ICIEM)*, Apr. 2021, pp. 211–215.
[94] A. Shehadeh, O. Alshboul, R. E. Al Mamlook, and O. Hamedat, "Machine learning models for predicting the residual value of heavy construction equipment: An evaluation of modified decision tree, LightGBM, and XGBoost regression," *Autom. Construct.*, vol. 129, Sep. 2021, Art. no. 103827.
[95] V. L. Deringer, A. P. Bartók, N. Bernstein, D. M. Wilkins, M. Ceriotti, and G. Csányi, "Gaussian process regression for materials and molecules," *Chem. Rev.*, vol. 121, no. 16, pp. 10073–10141, Aug. 2021.
[96] Q. Shi, M. Abdel-Aty, and J. Lee, "A Bayesian ridge regression analysis of congestion's impact on urban expressway safety," *Accident Anal. Prevention*, vol. 88, pp. 124–137, Mar. 2016.
[97] V. Vovk, "Kernel ridge regression," in *Empirical Inference: Festschrift in Honor of Vladimir N. Vapnik*. Berlin, Germany: Springer, 2013, pp. 105–116.
[98] D. H. Young and S. T. Bakir, "Bias correction for a generalized log-gamma regression model," *Technometrics*, vol. 29, no. 2, pp. 183–191, May 1987.

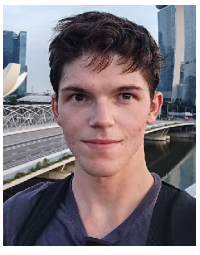

IVAN P. MALASHIN received the B.S. degree in technical physics from Bauman Moscow State Technical University (BMSTU), Moscow, Russia, in 2022, where he is currently pursuing the M.S. degree.

He is a Research Assistant with the Artificial Intelligence Research and Education Center, BMSTU. His research interests include developments in machine learning and its application for cyber-physical systems.

DANIIL S. DAIBAGYA is currently a Junior Researcher with the P. N. Lebedev Physical Institute, Russian Academy of Sciences. His research interest includes the studies of luminescent properties of colloidal nanoparticles.

VADIM S. TYNCHENKO (Senior Member, IEEE) was born in Kyiv, in 1985. He received the B.S. and M.S. degrees in systems analysis and operations research, in 2006 and 2008, respectively, and the Ph.D. degree in engineering from the Reshetnev Siberian State University of Science and Technology, Krasnoyarsk, Russia, in 2008. He is currently a Chief Researcher with the Artificial Intelligence Technology Scientific and Education Center, Bauman Moscow State Technical University, and a Professor with the Information and Control Systems Department, Reshetnev Siberian State University of Science and Technology. He is the author of more than 200 scientific articles and more than 20 inventions. His research interests include intelligent control systems, reliability improvement, and the management of technical objects and processes.

VLADIMIR A. NELYUB received the master's degree in engineering and technology from Bauman Moscow State Technical University, Moscow, Russia, in 2006, and the Ph.D. degree in chemistry from the Mendeleev University of Chemical Technology, Moscow, in 2016. He is currently a Vice-Rector for scientific affairs with Far Eastern Federal University and a Professor with the Scientific Department, Bauman Moscow State Technical University. His research interests include artificial intelligence, big data, advanced materials, and digital materials science.

ALEKSEI S. BORODULIN received the master's degree in engineering and technology from Bauman Moscow State Technical University, Moscow, Russia, in 2007, and the Ph.D. degree in chemistry from the Mendeleev University of Chemical Technology, Moscow, in 2016. He is currently the Director with the Scientific and Educational Center "Artificial Intelligence Technologies," Bauman Moscow State Technical University. His research interests include advanced materials and digital materials science, machine learning, soft matter, and management of technical objects and processes.

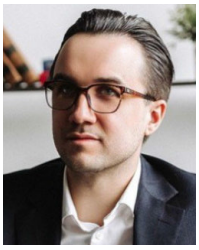

ANDREI P. GANTIMUROV received the M.S. degree from BMSTU. He is currently the Co-Founder and a Developer at a data storage systems company. He is also a Research Associate with BMSTU. His expertise lies in the design and implementation of innovative data storage solutions, where he has contributed significantly to the advancement of storage technology. He has been actively involved in research and development projects aimed at improving data storage efficiency and reliability. His work has been recognized for its impact on the field. He continues to drive innovation in the domain of data storage systems.

SERGEY A. AMBROZEVICH is currently a Senior Researcher with the P. N. Lebedev Physical Institute, Russian Academy of Sciences. His research interests include the studies of the optical properties of organic and organometallic phosphors.

ALEXANDR S. SELYUKOV is currently a Junior Researcher with the P. N. Lebedev Physical Institute, Russian Academy of Sciences. His research interest includes the studies of electroluminescent properties of colloidal nanocrystals.